European Geothermal Congress 2013
Pisa, Italy, 3-7 June 2013

Flow channelling in EGS reservoir: from fracture aperture variability to large scale deformation

K. Marakchi[1], V. Magnenet[2], J. Schmittbuhl[1], A. Genter[3], C. Fond[2], D. George[2], S. Ahzi[2]

[1] EOST, Université de Strasbourg/CNRS, France
[2] ICUBE, Université de Strasbourg/CNRS, France
[3] GEIE EMC, Route de Soultz-sous-Forêts, KUTZENHAUSEN

Mail: amarakchi@unistra.fr , EOST, Bâtiment Descartes - 5, rue René Descartes - F-67084 Strasbourg cedex
Tel: +33 3 68 85 00 90

Keywords: EGS, finite element modelling.

ABSTRACT

Using a finite element approach, we propose a numerical model to compute the large scale deformation of the Soultz-sous-Forêt HDR reservoir. In this first approach, only mechanical aspects are addressed and the behaviour of rocks is considered elastic and isotropic. We detail the simplified geometry and the boundary conditions used for the simulation and we finally discuss some perspectives.

1. INTRODUCTION

Soultz-sous-Forêts is located on the western edge of the Rhine Graben in the Pechelbronn oil field and has been exploited by many wells from the 19th century until 1964. This oil field showed the existence of a strong temperature gradient in the sedimentary layers. At Soultz-sous-Forêt, there is actually an important thermal gradient in the sedimentary cover (Triassic to tertiary, 1400 meters thick) up to 100 ° C / km [Ledésert et al., 1996], identified from measurements in the oil field of Pechelbronn [Hass and Hoffmann, 1926; Schnaebele, 1948; Sittler, 1972]. The thermal gradient measured in the crystalline basement decreases because of hydrothermal convective circulations from 1700 to 3500 meters . below the gradient is becoming more normal with 35 ° C / km [Pribnow et al., 1999].

Enhanced geothermal systems are geothermal reservoirs that have been engineered to increase the permeability and/or porosity of the geothermal resources. At Soultz-sous-Forêt, for instance, the hydraulic connection between the injection wells GPK1/GPK3 and the production wells GPK2/GPK4 has been improved by several hydraulic or chemical stimulations [Fritsch et al., 2007, Genter et al 2010]. Since 2006, the Soultz site has been operated to produce electricity since 2008. The fluid which circulates in a closed loop, is reinjected at a temperature of about 70 °C in GPK1 and GPK3 and is pumped into GPK2 and GPK4 at a temperature of about 150-160 °C at the wellhead [Genter et al., 2009]. This heat is converted by an ORC power plant d into electricity and distributed to the grid.

Several authors have built models of Soultz reservoir. Blumenthal et al. (2007) propose a simple 2D model taking into account the major structural units and a number of parameters as low as possible in order to limit the number of degrees of freedom (permeability, porosity). Sausse et al. (2010) create a deterministic 3D model of the fracture zone observed in the granitic reservoir of the Soultz reservoir. Baujard et al (2005) made a numerical study of the influence of the fluid density on the pressure distribution and the stimulated volume in the Soultz HDR reservoir. The main goal of all published models is to understand the hydro-thermo-chemical behavior of the reservoir in order to improve production and exploitation.

One of the problems currently encountered in the field of EGS exploitation is the channeling of water flow through fractures. This channeling induces preferential flow channels which greatly reduce the heat exchange between the brine and the host rock. The aim of our work is to study the influence of channeling on the system performance. To achieve this, we propose a finite element numerical modeling of the reservoir, which must integrate mechanical, thermal, hydraulic couplings. The model will be calibrated by a number of experimental data, borehole and field observations. In this first contribution, we focus on the mechanical modeling of the Soultz-sous-Forêt reservoir, considering only a mechanical loading on the major fault through wells GPK2 and GPK4.

This paper is organized as follow. In section 2, we introduce and explain the model and we show preliminary results. In section 3, we draw preliminary conclusions and describe the future works.

2. NUMERICAL MODEL

The first objective of our modeling is to calculate the displacement field at the ground surface when the

fault undergoes a shear offset of several centimeters at depth, as measured in [Cornet et al. 1997]. The aim of this calculation is to interpret InSAR measurement (unpublished work of C. Heimlich, et al., (2013) who do a geodetic survey of the geothermal sites of Soultz-sous-Forêts and Rittershoffen (Upper Rhine Graben - France).

2.1 Reservoir mesh

Our model consists of a cube within the upper crust of 10 km in size, containing two layers: a sedimentary layer between 0 m and 1450 m depth and a granitic layer between 1450 m and 10000 m depth. The geometrical description of the fault, approximated by an ellipse intersecting the granite layer only, is taken from [Sausse et al. 2010] and [Cornet 2007]. More precisely, geometrical parameters are listed in Tab.1.

Tab. 1 Structural and geometrical data of the major fault defined from well-logging analysis [Sausse et al. 2010]

Extension of major axis	3000m
Extension of minor axis	3000m
Dip direction	234°
Dip	71°
Thickness	10m

Only two perfectly vertical boreholes of 20 cm in diameter are taken into account in this first approach. In future simulations including hydraulic aspects, the first one will be considered as a producer while the second one will be an injector. The entire geometry of the model is shown in Figure 1. The commercial finite element software Abaqus © has been used for the design of the geometry and for the simulations.

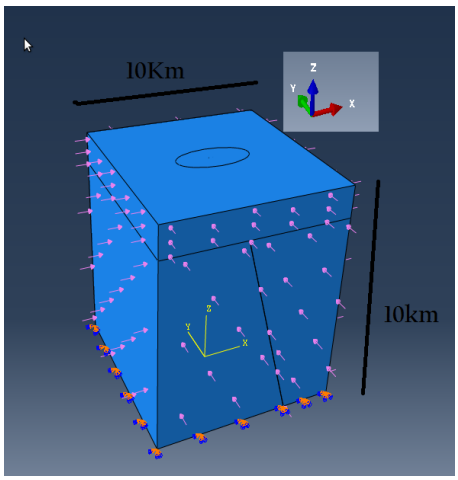

Figure 1 : Geometry of the model and load. This figure shows the geometry of the model. It is cube 10x10x10 km3. The main fracture of the reservoir is included. The loading on the edges are those proposed by Cornet et al (2010), see paragraph 2.3.

The mesh consists of 259 483 nodes and 185 866 elements C3D10 type (pyramids with 10 nodes). Each node of the mesh is associated with three degrees of freedom corresponding to the displacement field components $\vec{U} = \{U_1, U_2, U_3\}$, cf. figure 2.

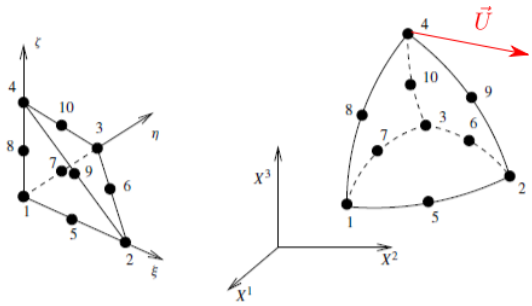

Figure 2: Type of elements used in the simulation (left: reference element, right: deformed element)

The 10-node tetrahedral element is characterized by quadratic interpolation function within the element. The local coordinate system is the same as for the 4-node tetrahedral element. The shape functions in the reference space described by the variables (ξ, η, ζ) take the form:

$$\begin{aligned}
\varphi_1 &= [2(1-\xi-\eta-\zeta)-1][1-\xi-\eta-\zeta] \\
\varphi_2 &= (2\xi-1)\xi \\
\varphi_3 &= (2\eta-1)\eta \\
\varphi_4 &= (2\zeta-1)\zeta \\
\varphi_5 &= 4(1-\xi-\eta-\zeta)\xi \\
\varphi_6 &= 4\xi\eta
\end{aligned} \qquad (1)$$

The mesh is shown in Fig. 3.

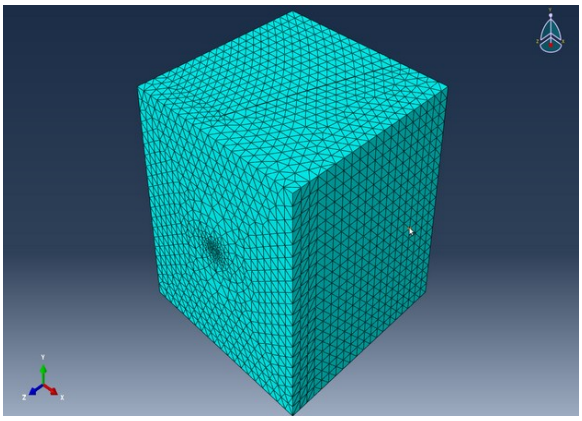

Figure 3: Mesh used for the simulation (the refined zone on the left correspond to the vicinity of the boreholes). In this figure we rotated the axes to show the mesh around wells

2.2 Constitutive equations and material properties

The rock is considered as an isotropic and elastic material, and the sole volume force taken into account is the gravity $\vec{g}$. Under these assumptions, the equations relating the Cauchy stress tensor $\overline{\overline{\sigma}}$, the strain tensor $\overline{\overline{\varepsilon}}$ and the displacement field $\vec{U}$ read:

$$\begin{aligned} &\overrightarrow{div}\,\overline{\overline{\sigma}} + \rho\vec{g} = \vec{0} \\ &2\,\overline{\overline{\varepsilon}} = \overline{\overline{\nabla}}\vec{U} + \overline{\overline{\nabla}}\vec{U}^{T} \\ &\overline{\overline{\varepsilon}} = \left(\frac{1+\nu}{E}\right)\overline{\overline{\sigma}} - \left(\frac{\nu}{E}\right)Tr(\overline{\overline{\sigma}})\,\overline{\overline{I}} \end{aligned} \qquad (2)$$

With E the Young modulus, ν the Poisson ratio, and $\overline{\overline{I}}$ the unit tensor. After discretization of the displacement field in terms of shape functions, these equations reduce to a linear system involving the nodal displacements. Properties of the materials are chosen as typical values for the Young modulus, the Poisson ratio, and the density (see Tab. 2.)

Tab. 2. Mechanical properties of the considered materials

Materials	Mass density (Kg/m^3)	Young's modulus (GPa)	Poisson's Ratio
Sediments	2900	30	0.3
Granite	2900	30	0.27
Fault zone	1000	10	0.2

The whole simulation is carried out in time steps of 1s, the value of the latter being totally insignificant since the materials obey a time independent behaviour. The CPU time taken to carry out the simulation is close to 2h40 on a regular PC.

2.3 Boundary and loading conditions:

To supplement the constitutive equations described in the previous section, a set of boundary conditions has to be prescribed. Firstly, the displacement field is assumed to vanish at the bottom of the cube. On the sides, the stress field proposed by Cornet et al (2007) has been considered and implemented as:

$S_h = 15.1 + 0.0179\,(z - 1458)$ (3a)

$S_H = 15.1 + 0.0179\,(z - 1458)$ (3b)

$S_v = 0.024z$ (3c)

In Eq. (3) S_H, S_h and S_v are, respectively, the minimum horizontal, the maximum horizontal, and the vertical principal stress component (MPa) while z is the depth (in meters). On the top of the cube, the stress vector vanishes because of the free boundary condition. Concerning the loading conditions, a shear displacement (about 4cm in magnitude) is applied to the footwall of the fault. This displacement corresponds to the displacement measured by Cornet et al. (1997), and is shown in Fig. 4.

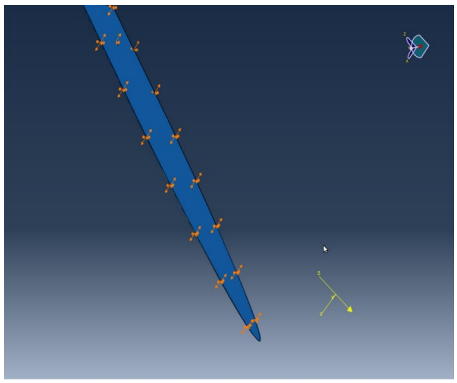

Figure 4: Boundary condition for the fracture, this figure represents only the fault (dip 71 °) and shows the boundary conditions applied on the fault. Namely, we set an offset between the lower footwall and the upper footwall of 4 cm.

2.4 Post Processing:

At the end of the simulation, the displacement field can be calculated on the top of the cube, corresponding to the ground surface and compared to the displacement field at the state of equilibrium (without fault displacement), see e.g. Fig. 5.

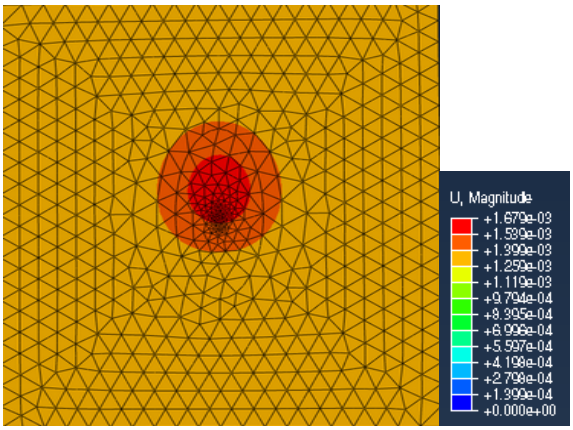

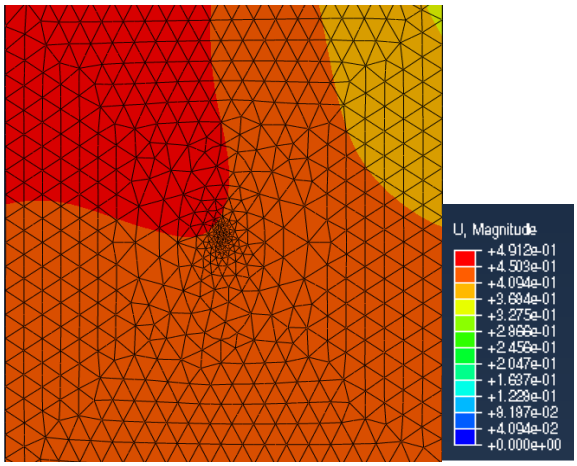

Figure 5: Magnitude of displacement (cm) field on the ground surface as calculated by the finite elements simulation. The first figure shows displacement on surface at the state of equilibrium. The second figure shows the calculated surface displacement when the fault offset is 4 cm along theprincipal fault axis direction.

In this figure we see that, in equilibrium, we can see a displacement of the order of 1.7 10-3 cm. In the second case (4 cm displacement for fault) we observe about 0.5cm displacement in the ground surface. Our purpose is to compare this displacement field at the ground surface with InSAR data in order to interpret InSAR measurements.

3. FORTHCOMING WORKS

3.1 Improving of the geometry

At this stage, only two straight boreholes have been considered, but the boreholes are actually curved. In the same spirit, only one fault has been considered in comparision with the 32 fault and fractures that have been identified in Sausse et al. (2010), see Fig. 6. One of the main challenge is to take into account the all the faults and to mesh their intersections.

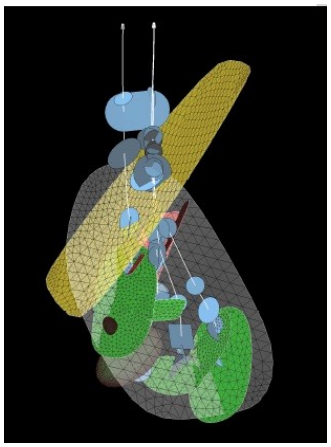

Figure 6: 3D Geological reservoir model created by Sausse et al. (2010) and Place et al. (2011).

3.2 Hydraulic and thermal aspects

Our second objective is to integrate hydraulic and thermal aspects in the simulations, given that these aspects have a great impact on the efficiency of the reservoir. On this topic, Neuville et al (2010) examined the influence of fracture roughness on hydraulic permeability and heat flux through the sides of a fracture when a cold fluid is injected into a hot fracture. They studied spatial temperature fluctuations inside the fluid assuming the temperature of the rock to be constant and the fracture aperture to be multi-scale. The main conclusion of the authors is that fingering of the flow or channeling is due to the fact that the aperture a may be varying in the plane of the fault with strong spatial correlations, see Fig. 7.

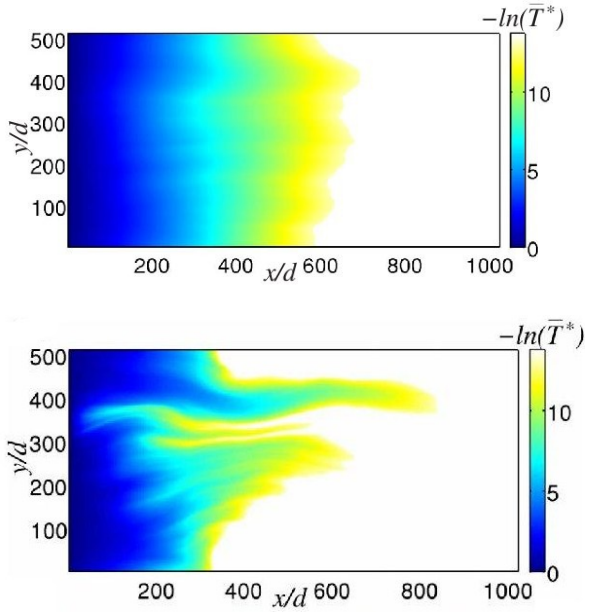

Figure 7: Fluid flow in a self-affine fracture. Top: σ/A=0.05, bottom: σ/A=0.25 (σ/A is the standard deviation of roughness divided by mean aperture) [Neuville et al. 2010]

To take into account the channeling phenomenon at the reservoir scale, specific finite elements representative of fault will be implemented. The specificity of these elements is that they contain nodes associated with fluid degrees of freedom (pressure P and temperature T) located between the footwall of the fault associated with mechanical degrees of freedom only, see Fig. 8.

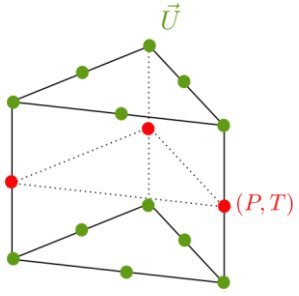

Figure 8: Specific finite elements representative of faults: the green nodes are relative to the footwall of the fault while the red nodes are relative to the fluid inside the fault.

The governing equations of these elements will be the same equations as the equations solved by Neuville et al. (2010), that is:

$$div_2(a^3 \nabla_2 p) = 0 \quad (4)$$

$$q.\nabla_2 \overline{T} + \frac{2\chi\alpha}{a}(\overline{T} - T_r) = 0 \quad (5)$$

$$q = a v_{moy} = \int_{z_1}^{z_2} v dz = -\frac{a^3}{12\eta} \nabla_2 p \quad (6)$$

with $a(x,y)$, $p(x,y)$, $v(x,y)$ the aperture, the pressure head, and the velocity of the fluid in the plane of the fault, χ the diffusivity of the fluid, α a coefficient measuring the efficiency of the heat exchange between the fluid and the rock, η the dynamic viscosity of the fluid and $\overline{T}$, T_r the temperature of the fluid and rock respectively. This kind of elements will be useful to simulate the fault behavior at the reservoir scale.

3.3 Sensitivity analysis

The main interest of having a complete thermo-hydro-mechanical model of the reservoir is to quantify the effect of the input parameters (such as the temperature, pressure and flow in the injection shaft or mechanical properties of materials inside the reservoir) on the output quantities (such as the flow enthalpy) in the production well. On the mathematical viewpoint, it consists in varying one value of an input parameter, leaving all the others parameters unchanged and to evaluate the resulting variation on the output variables. The aim of this study is first to identify the most influential input parameters on which an optimization procedure could be carried out. In addition, this analysis could reveal irrelevant parameters in the sense that non-sensitive parameters do not need to be known exactly.

3. CONCLUSIONS

To integrate the effect of channelling phenomena at the reservoir scale, we develop a fully thermal, hydraulic and mechanical coupled simulation. At this stage, the mechanical model is almost finished, but needs to be compared (using back analysis) to InSAR data. The thermal and hydraulic effects are currently being integrated into this first mechanical model. Our aim is to study the sensitivity of input parameters. The second step of the work will be to improve the geometries (e.g. using the real well direction), to include flow channelling within fractures and to include all the faults identified in the reservoir.

ACKNOWLEDGEMENTS

This work was done in the framework of the Labex G-EAU-THERMIE PROFONDE which was funded by the French government under the program "Investissements d'Avenir".

REFERENCES

Al-Yaarubi, A., Pain, C., Grattoni, C. and Zimmerman, R. : Dynamics of Fluids and Transport in Fractured Rocks, AGU Monograph Vol. 162, American Geophysical Union, Washington, D.C., 2005, 55–64.

Baujard, C. , Bruel,, D., Numerical study of the impact of fluid density on the pressure distribution and stimulated volume in the Soultz HDR reservoir, *Geothermics* 35, 2006, 607–621

Bachler, D., Kohl, T., Rybach, L.: Impact of graben parallel faults on hydrothermal convection – Rhine graben case study *Physics and Chemistry of the Earth, Parts A/B/C* Volume 28, Issues 9–11, 2003, Pages 431–441

Baujard, C.and Bruel, D.: Improving a numerical tool and evaluating impact of density charge of injected fluid in the behaviour of HDR reservoir, *Processing of the 30th Workshop on geothermal reservoir engineering*, 2005.

Cornet, F.: The relationship between seismic and assesmic motion induced by forced fluid injection, *Hydrogeology journal* 20, 2012, 1463-1466.

Cornet, F., Bérard, T., Bourouis, S.: How to close to failure is a granite rock mass at depth?, *International Journal of Rock Mechanics & mining Science* 44, 2007, 47-66.

Cornet, F., Helm, J., Pointrenaud, H. and Etchecopar, A.: Seismic and Aseismic Slips Induced by Large-scale Fluid Injections, *Pure and applied geophysics* 150, 1997, 563-583.

Fritsch, D., Baumgaertner, J., Cuenot, N., Gra, J. and Genter, A.: *Synthèse des travaux du projet Soultz. Technical report, BRGM.* Note traduite de la présentation : "The Soultz EGS pilot plant : energy heat and power from deep Enhanced Geothermal Systems", 2008, Monte-Carlo (Monaco)

Genter, A., Evans, K., Cuenot, N., Fritsch, D., Sanjuan, B.: Contribution of the exploration of deep crystalline fractured reservoir of Soultz to the knowledge of enhanced geothermal system (EGS), *C.R. Geoscience*, 342 (2010) 502-516.

Gérard, A., Genter, A., Kohl, T., Lutz, P., Rose, P. and Rummel, F.: The deep EGS (Enhanced Geothermal System) project at Soultz-sous-Forêts

(Alsace, France). *Geothermics*, 2006, 35(5-6) :473.

Kohl, T., Evans, K.F., Hopkirk, R.J and Rybach, L.: Coupled hydraulic, thermal and mechanical consideration for the simulations of hot dry rock reservoirs, *Geothermics*, Vol 24, N°3, 1995, 345-359

Méheust, Y.and Schmittbuhl, J.: Flow enhancement of a rough fracture. *Geophysics Research Letters*, 2000, 27:2989-2992.

Neuville, A., Toussaint, R., Schmittbuhl, J.: Fracture roughness and thermal exchange : A case study at Soultz-sous-Forêts.*Comptes Rendus Geoscience* 342, 2010, 616-625.

Roux, S., Plouraboué, F., and Hulin, J-P.: Tracer dispersion in rough open cracks.*Transport in Porous Media*,1998, 32(1) :97-116.

Sausse, J., Dezayes, C., Dorbath, L., Genter, A., Place, J.: 3D model of fracture zones at Soultz-sous-Forets based on geological data, image logs, induced microseismicity and vertical seismic profiles, *Comptes Rendus Geoscience 342* , 2010, 531–545

Zimmerman, R.and Yeo, I-W.:Geophysical Monograph *American Geophysical Union*, Washington, D.C., 2000, Vol. 122, p. 213.